Islamic Azad University

Journal of

Optoelectronical Nanostructures

Winter 2019 / Vol. 4, No. 1

Thermal Annealing Influence over Optical Properties of Thermally Evaporated SnS/CdS Bilayer Thin Films

Zahra Dehghani Tafti[1], Mahmood Borhani Zarandi[*,2], Hojjat Amrollahi Bioki[2, 3]

[1] Department of Physics, Faculty of Basic Sciences, Payame Noor University, Tehran, Iran

[2] Atomic and Molecular Group, Faculty of Physics, Yazd University, Yazd, Iran

[3] Department of Physics, Tarbiat Modares University, Tehran, Iran

(Received 22 Dec. 2018; Revised 12 Jan. 2019; Accepted 25 Feb. 2019; Published 15 Mar. 2019)

Abstract: Thin films of tin sulfide/cadmium sulfide (SnS/CdS) were prepared by thermal evaporation method at room temperature on a glass substrate and then annealed at different temperature with the aim of optimizing the optical properties of the material for use in photovoltaic solar cell devices. The effect of annealing on optical properties of SnS/CdS film was studied in the temperature range of 100 to 400 °C with steps of 100 °C. The films were characterized by optical absorption spectra. The optical constants such as band gap, refractive index (n) and extinction coefficient (k) were calculated on different annealing temperature and in the wavelength range of 250 nm to 750 nm. Analysis of the optical absorption coefficient demonstrated the presence of direct optical transition and the corresponding band gap values showed enhancement as deposition annealing temperature increased. The energy band gap in the range 2.20 eV – 3.18 eV has been obtained for a film as-deposited which increases clearly with increasing annealing temperature. The refractive index and extinction coefficient both decrease notably with increasing annealing temperature.

Keywords: CdS, Optical Properties, SnS, Thermal Annealing, Thin Film, Vacuum Evaporation.

1. INTRODUCTION

In recent years, thin films of tin sulfide (SnS) have attracted much attention for photovoltaic applications due to high absorption coefficient ($\approx 10^4$ cm^{-1} near the fundamental edge) and high conductivity (hole mobility = 90 $cm^2V^{-1}s^{-1}$) [1]. SnS belongs to groups IV-VI of compounds with Sn as a cation and S as an anion. The constituent elements are often inexpensive, nontoxic and abundant in nature leading to the development of devices that are environmentally friendly and have public acceptability. The optoelectronic properties of SnS is also an

* Corresponding author. Email: mborhani@yazd.ac.ir

important material that is found in zinc blend with the lattice constant (a=0.5845 nm), orthorhombic with the lattice constants (a=0.385 nm, b=1.142 nm, and c=0.438 nm) and herzenbergite crystal structures [2]. Furthermore, it usually exhibits band gap of 1.0 to 1.1 eV for the indirect transition and about 1.2 to 1.5 eV for the direct transition with a high absorption coefficient above the fundamental absorption edge [3]. It could be used to build photovoltaic p–n or p–i–n structures with conversion efficiencies of about 25% [3-6].

Among II-VI semiconductors, cadmium sulfide (CdS) polycrystalline thin films have a wide range of applications such as large area electronic devices and solar cells and because of their wide direct band gap (2.42 eV) they have been used as a window material together with several semiconductors such as CdTe, Cu_2S and $CuInSe_2$ [7, 8]. The interest toward using CdS thin films also originates from its piezoelectric properties and potential laser applications [9]. Many deposition techniques are used for fabrication of SnS and CdS thin films such as vacuum evaporation [3], sputtering [10] and chemical methods such as chemical vapor deposition (CVD) [11]. Every technique of thin film deposition has its own advantages and disadvantages.

At present work, SnS/CdS thin films prepared by vacuum evaporation technique at room temperature. Then thin films submitted to the different annealing temperature in order to improve optical and morphological properties. We have determined the effect of annealing temperature on optical properties of SnS/CdS thin films, deposited by the evaporation technique.

2. EXPERIMENTAL DETAILS

A. Chemicals

For sample preparation, 15.0 g $SnCl_2$, $2H_2O$ was dissolved into 100 ml deionized water, and while heating a few drops of HCl were added to make an acidic environment for the better reaction. In another test tube, 50 ml $(NH_4)_2S$, 1.5 M was dissolved into 100 ml deionized water, and then two solutions were mixed together under ventilator at 60 °C for 1 h. After collecting the black deposit by filter paper, it was dried overnight in the oven at 60 °C.

B. Deposition of SnS/CdS thin films

The deposition of SnS thin films was performed in conventional vacuum thermal evaporator using VAS-BUC coating unit (Model 78535-France). The substrates used for deposition without heating was soda-lime glass substrate (SLG) that was ultrasonically cleaned by propanol solution for 10 min and following the rinse with deionized water, it was dried with acetone for three times. The SnS powder as a source was placed in the molybdenum boat-type heater. Then the evaporation process was done at 10^{-5} mbar pressure and 1260°C, with rot speed 800 rph and deposition rate 0.1 nm s^{-1} for 15 minutes.

After that, CdS granule with 99.99٪ purity supplied by Jiangyan ATS Optical Material Co., Ltd. deposited on glass substrate by a tungsten boat was used as a support to evaporate on SnS thin films at 10^{-5} mbar and 1750 °C, with rot speed 900 rph and deposition rate 0.2 nm s^{-1}.

The film thickness was measured 213 nm by a quartz crystal monitor (Model FTM6) mounted near the substrate for in-situ measurements of the thickness of the thin films as well as the evaporation rate, deposition process. Subsequently, the SnS/CdS samples were annealed in atmosphere at 100, 200, 300, and 400 °C respectively for 60 min in a tube furnace.

C. Characterization of the films

The optical constants and absorption spectra of thin films were measured by UV/Vis spectrophotometer (CINTRA101, Yazd University) at wavelength range from 350 to 750 nm. The surface morphology measurements were performed using a scanning electron microscope (SEM, VEGA2, TESCAN, Czech).

3. RESULTS AND DISCUSSION

The SEM images of the SnS/CdS thin films: (a) as-deposited and (b) annealed at 300 °C shown in Fig. 1 illustrate uniform, continuous and dense microstructures. The grains consisted of several crystallites and with the increase of annealing temperatures the film growth proceeds through agglomeration of the islands. These islands later coalesced together to form the continuous film with a further increase of temperature [12], leading to a homogeneous close-packed surface, consisted of rice-shaped grains. The grain size was 20 nm that increased with increasing annealing temperature.

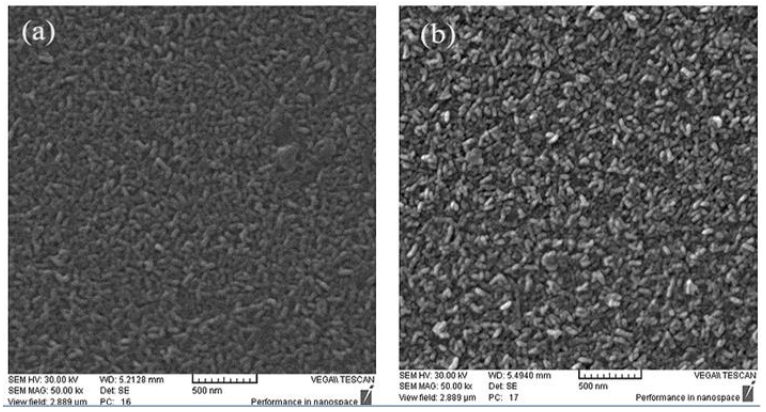

Fig. 1. SEM morphology of the SnS/CdS thin films: (a) as-deposited and (b) annealed at 300 °C.

Optical Absorbance spectra of the SnS/CdS thin films were characterized and the optical absorption coefficient α was evaluated using the following equation [13],

$$\alpha = -\frac{1}{t}\ln(T) = 2.303\frac{A}{t} \quad (1)$$

which, T is transmittance, A is absorbance and, t is the film thickness. Fig. 2, shows absorbance spectra of SnS/CdS thin films with different annealing temperature. The bilayer of SnS and CdS, increased the absorption of samples, compared with cadmium sulfide and included a greater range of the visible spectrum. The maximum absorption coefficients of all the thin films are greater than 10^5 cm^{-1} that expresses thin films was strong absorbance layer. As shown in Fig. 2, the absorption decreases with increasing annealing temperature. At short wavelength, the annealed films at higher temperature have lower absorbance. It is argued that when temperature increase, grain size and inter granular spaces increases and it leads to reduction of absorbance as a consequence (perhaps due to increasing transmittance) [14] . Absorption edge has blue shift with annealing and it's due to the increase of grain size [15, 17]. However, when the annealing temperature is equal to or greater than 300°C, the absorption coefficient decreases rapidly that probably due to the presence of SnO_2 in the films.

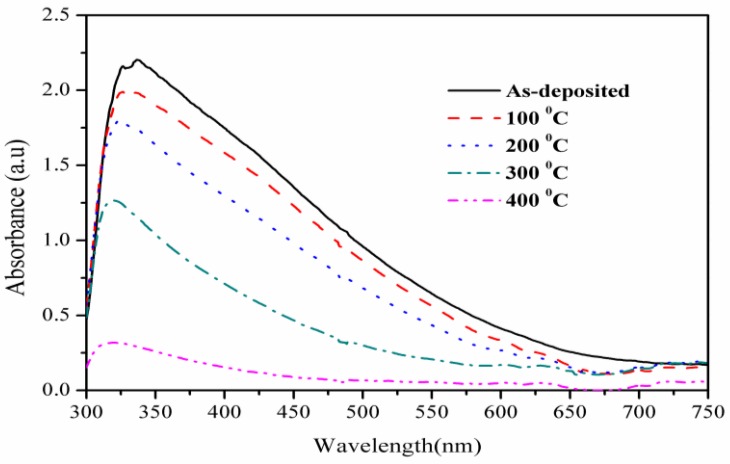

Fig. 2. Absorbance spectral of SnS/CdS thin films annealed at the different temperature.

The relation between the absorption coefficient, α, and the incident photon energy, $h\nu$, is given by tauc equation [18],

$$\alpha h\nu = B(h\nu - E_g)^m \quad (2)$$

where *B*, is constant characteristic parameter independent of photon energy and *m* is a constant which depends on the nature of the transition between the top of the valence band and bottom of the conduction band can have values 1/2, 2, 3/2 and 3 for allowed direct, allowed indirect and forbidden direct and indirect transitions respectively.

The value of optical band gap energy (E_g) for different annealing temperature of thin films can be obtained from the graph of $(\alpha hv)^2$ versus hv, by extrapolating the liner portion of the plot $(\alpha hv)^2$ versus hv to α=0. The curve has a good straight-line fit over the higher-energy range above the absorption edge indicative of a direct optical transition near the absorption edge. Fig. 3, shows $(\alpha hv)^2$ versus hv curve of the as-deposited and annealed SnS/CdS thin films at different annealing temperature. The inset shows the direct band gap of SnS/CdS bilayer thin film about 3.18 eV annealed at 400 °C. For annealing films at 200 °C, the band gap is 2.42 eV is as same as the CdS bulk. The calculated band gap values are shown in Table 1. The changes of band gap with increasing annealing temperature are caused by changes in the defects, the composition and the crystalline properties of the CdS and SnS thin films. The results significantly has high concordance with other research in optical properties of bilayer thin film fields [19, 20]. It is observed that the band gap increases as the annealing temperature increase which can be due to the Burstein-moss effect is related to the carrier concentration was increased [17, 21]. This increment could be attributed to the increase in crystallite size, which induced a decrease in dislocation density. At high annealing temperature, the increase of the band gap value could be due to the loss of the sulfur and the formation of oxides. It is evident that an increase in the annealing temperature fairly effects on the mobility of charge carriers. Grain boundaries with high defect densities act as scattering centers, and hence, significantly reduce the carrier mobility. Due to small crystallite size, in the as-deposited films, carriers have to travel multiple grain boundaries, resulting in low mobility [17].

Table 1. Optical band gap and Urbach Energy values of SnS/CdS thin films at the different annealing temperature

Annealing Temperature (°C)	*Energy gap (eV)*	*Urbach energy (eV)*
As-deposited	2.20	1.22
100	2.28	1.24
200	2.42	1.30
300	2.72	1.35
400	3.18	1.21

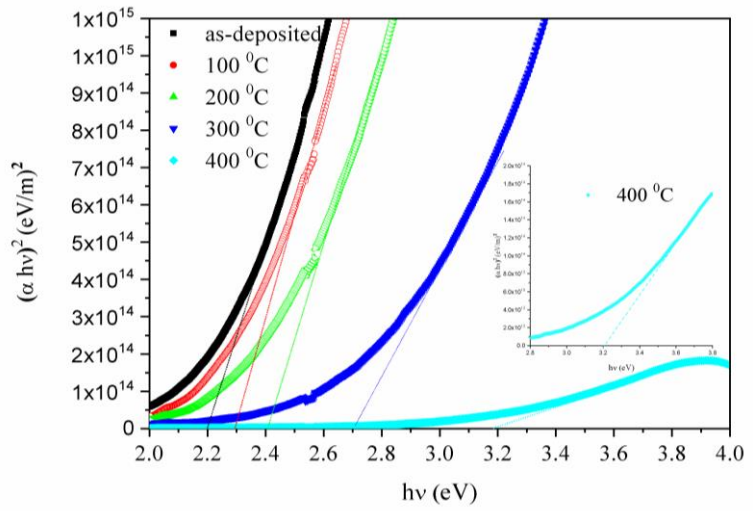

Fig. 3. Plot of $(\alpha h\nu)^2$ vs. hν for SnS/CdS thin films prepared at the different annealing temperature. Inset figure presents $\alpha h\nu)^2$ vs. hν relation for SnS/CdS thin film annealed at 400 °C in large scale.

The Urbach tail energy in annealed SnS/CdS thin films can be determined by the following relation [22];

$$\alpha = \alpha_0 \exp \frac{h\nu}{E_u} \tag{3}$$

where α is absorption coefficient, $h\nu$ is the photon energy, α_0 is constant and E_u is the Urbach energy, which refers to the width of the exponential absorption edge amorphous semiconductors [23]. The Urbach tail energy, E_u, is calculated from the slope of $\ln\alpha$ versus the photon energy plot. For an ideal semiconductor, the Urbach energy is zero so the slope is infinite. The higher the Urbach energy, the wider is the region below band gap with a significant amount of tail absorbing states [24]. Fig. 4, shows the variation of $\ln\alpha$ versus photon energy for SnS/CdS thin films before and after annealing at the different temperature. The values of E_u are given in Table 2, which indicates the Urbach Energy values increase with the increase in annealing temperature up to 300 °C. This indicates that the crystalline nature of the thin films increases with the increase in film annealing temperature. The decrease Urbach Energy values are slightly more as the annealing temperature increases to 400 °C which indicates an improvement in the quality of SnS/CdS thin films on annealing.

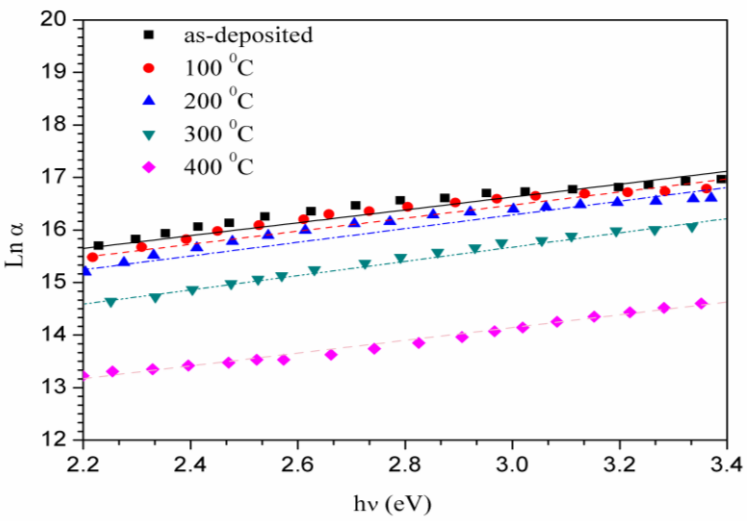

Fig. 4. The dependence of the Lnα on photon energy for SnS/CdS thin films at the different annealing temperature.

Optical parameters namely refractive index, n, and extinction coefficient, k, have been calculated from transmittance measurements using Swanepoel equation [25],

$$n = \left[N^2 - (N^2 - s^2)^{1/2} \right]^{1/2} \tag{4}$$

Where

$$N = 2s \frac{T_{\max} - T_{\min}}{T_{\max} \times T_{\min}} + \frac{s^2 + 1}{2} \tag{5}$$

and *s*, is the substrate refractive index (s=1.52 for glass), T_{max} is the maxima and T_{min} is the minima envelop curve of the transmission spectrum. The results showed that the refractive index was decreased from 2.57 to 1.61 at λ=550 nm by increasing annealing temperature up to 400 °C which is due to crystallinity improvement. On the other hand, the refractive index depends on the porosity and would be influenced by the surface roughness on the scale of the wavelength of the light. It can be seen from Fig. 1, with increment in annealing temperature the porosity was increased. The voids and porosities absorb, refract and diffract the light in various directions thereby decreasing the refractive index.

The absorption coefficient can be used to find the extinction coefficient by,

$$k = \frac{\alpha\lambda}{4\pi} \tag{6}$$

The refractive index and extinction coefficient of annealed SnS/CdS thin films, as a function of wavelength, are shown in Fig. 5 and Fig. 6. Obviously, when the crystalline quality is better and the crystallite size increases, both indices decrease with increasing annealing temperature [8, 13, 17]. The lowest refractive index is for the sample annealed at 300℃ and is about 1.70. The extinction coefficient is in order of 10^{-1}.

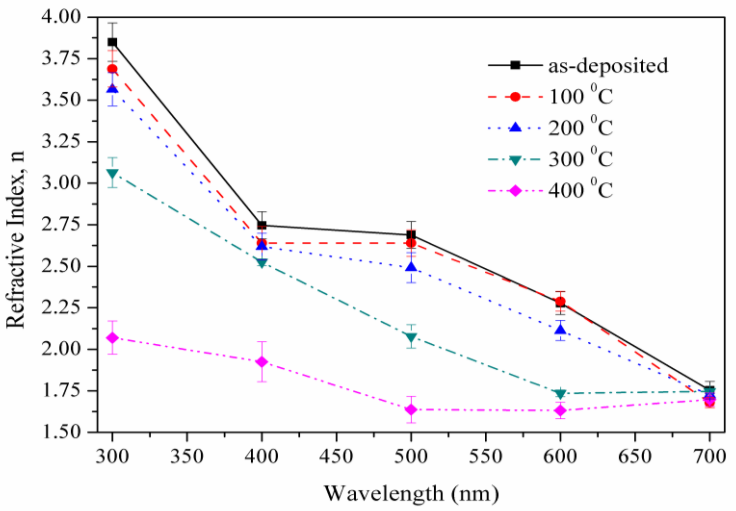

Fig. 5. Refractive index of annealed SnS/CdS thin films as a function of wavelength.

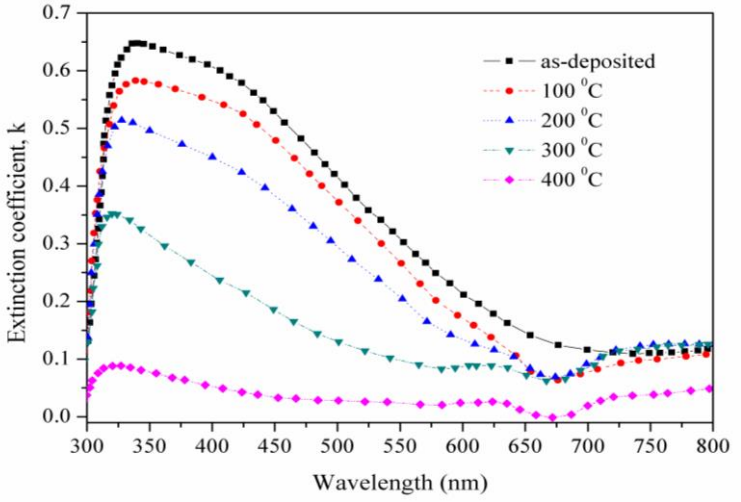

Fig. 6. Extinction coefficient of annealed SnS/CdS thin films as a function of wavelength.

4. CONCLUSION

SnS/CdS thin films were deposited by vacuum evaporation method and then were annealed at a temperature of 100, 200, 300 and 400 ℃, respectively. The results showed high absorption in the visible wavelength range and the absorption coefficient was in the order of 10^5 cm^{-1} that is suitable for solar cells applications. Annealing reduced the absorption by shifting the absorption edge to short wavelength and increased energy gap which was as a result of increase in grain size and blue shift in absorption edge. The film's surface was uniform, dense and rice-shaped. After annealing the grain size and uniformity increased at 300℃. Moreover, the refractive index of SnS/CdS thin film decreases with annealing temperature and the extinction coefficient decreases a little during the lower temperature anneal. The SnS/CdS thin film annealed at 300℃ has the best optical property and it may be optimal for thin film solar cells applications as a windows layer.

REFERENCES

[1] E. Guneri, F. Gode, C. Ulutas, F. Kirmizigul, G. Altindemir, C. Gumus. *Properties of p-type SnS thin films prepared by chemical bath deposition.* Chalcogenide Letters. 7 (12) (2010) 685-694.

[2] A. Mukherjee, P. Mitra. *Structural and optical characteristics of SnS thin film prepared by SILAR.* Materials Science-Poland. 33 (4) (2015) 847-851.

[3] S. Hegde, A. Kunjomana, M. Prashantha, C. Kumar, K. Ramesh. *Photovoltaic structures using thermally evaporated SnS and CdS thin films.* Thin Solid Films. 545 (2013) 543-547.

[4] A. Abdelrahman, W. Yunus, A. Arof. *Optical properties of tin sulphide (SnS) thin film estimated from transmission spectra.* Journal of non-crystalline solids. 358 (12) (2012) 1447-1451.

[5] S. Ahmed, L. Latif, A. Salim. *The effect of substrate temperature on the optical and structural properties of tin sulfide thin films.* Journal of Basrah Researches ((Sciences)) Volume. 37 (3A/15) (2011)

[6] E. Guneri, C. Ulutas, F. Kirmizigul, G. Altindemir, F. Gode, C. Gumus. *Effect of deposition time on structural, electrical, and optical properties of SnS thin films deposited by chemical bath deposition.* Applied Surface Science. 257 (4) (2010) 1189-1195.

[7] A. Mirkamali. *Numerical Simulation of CdS/CIGS Tandem Multi-Junction Solar Cells with AMPS-1D.* Journal of Optoelectronical Nanostructures. 1 (4) (2017) 31-40.

[8] W. Daranfed, M. Aida, N. Attaf, J. Bougdira, H. Rinnert. *Cu 2 ZnSnS 4 thin films deposition by ultrasonic spray pyrolysis.* Journal of Alloys and Compounds. 542 (2012) 22-27.

[9] M. Mahdi, S. Kasem, J. Hassen, A. Swadi. *Structural and optical properties of chemical deposition CdS thin films.* International Journal Nanoelectronics and Materials. 2 (2009) 163-172.

[10] M. Becerril, H. Silva-López, O. Zelaya-Angel, J. R. Vargas-Garcia. *Au doping of CdS polycrystalline films prepared by co-sputtering of CdS-Cd-Au targets.* Superficies y vacío. 25 (4) (2012) 214-217.

[11] R. Mane, C. Lokhande. *Chemical deposition method for metal chalcogenide thin films.* Materials Chemistry and Physics. 65 (1) (2000) 1-31.

[12] Y. V. Subbaiah, P. Prathap, K. R. Reddy. *Structural, electrical and optical properties of ZnS films deposited by close-spaced evaporation.* Applied Surface Science. 253 (5) (2006) 2409-2415.

[13] H. Alexander, H. Teichler. *Dislocations.* Materials science and technology. (1991)

[14] H. Izadneshan, G. Solookinejad. *Effect of Annealing on Physical Properties of Cu2ZnSnS4 (CZTS) Thin Films for Solar Cell Applications.* Journal of Optoelectronical Nanostructures. 3 (2) (2018) 19-28.

[15] V. G. Klyuev, D. V. Volykhin, O. V. Ovchinnikov, S. I. Pokutnyi. *Relationship between structural and optical properties of colloidal CdxZn1− xS quantum dots in gelatin.* Journal of Nanophotonics. 10 (3) (2016) 033507-033507.

[16] X.-Q. Zhang, J.-B. Chen, W.-D. Zhu, C.-W. Wang. *Enhanced field emission from hydrogenated SnO2 nanoparticles embedded in TiO2 film on fluorinated tin oxide substrate.* Journal of Vacuum Science & Technology B. 32 (2) (2014) 021808.

[17] M. Borhani Zarandi, H. Amrollahi Bioki. *Effects of Cobalt Doping on Optical Properties of ZnO Thin Films Deposited by Sol–Gel Spin Coating Technique.* Journal of Optoelectronical Nanostructures. 2 (3) (2017) 33-44.

[18] J. Tauc. *Optical properties and electronic structure of amorphous Ge and Si.* Materials Research Bulletin. 3 (1) (1968) 37-46.

[19] A. Abdel Haleem, M. Ichimura. *Experimental determination of band offsets at the SnS/CdS and SnS/InS x O y heterojunctions.* Journal of Applied Physics. 107 (3) (2010) 034507.

[20] A. Mirkamali, K. Muminov. *The effect of change the thickness on CdS/CdTe tandem multi-junction solar cells efficiency.* Journal of Optoelectronical Nanostructures. 2 (2) (2017) 13-24.

[21] K. Saw, N. Aznan, F. Yam, S. Ng, S. Pung. *New insights on the burstein-moss shift and band gap narrowing in indium-doped zinc oxide thin films.* PloS one. 10 (10) (2015) e0141180.

[22] C. Benouis, M. Benhaliliba, A. S. Juarez, M. Aida, F. Chami, F. Yakuphanoglu. *The effect of indium doping on structural, electrical conductivity, photoconductivity and density of states properties of ZnO films.* Journal of Alloys and Compounds. 490 (1) (2010) 62-67.

[23] S. Zaynobidinov, R. Ikramov, R. Jalalov. *Urbach energy and the tails of the density of states in amorphous semiconductors.* Journal of Applied Spectroscopy. 78 (2) (2011) 223-227.

[24] N. Prtljaga, D. Navarro-Urrios, A. Tengattini, A. Anopchenko, J. M. Ramírez, J. M. Rebled, S. Estradé, J.-P. Colonna, J.-M. Fedeli, B. Garrido. *Limit to the erbium ions emission in silicon-rich oxide films by erbium ion clustering.* Optical Materials Express. 2 (9) (2012) 1278-1285.

[25] R. Swanepoel. *Determination of the thickness and optical constants of amorphous silicon.* Journal of Physics E: Scientific Instruments. 16 (12) (1983) 1214.